Electron acceleration during streamer collisions in air

Köhn, Christoph; Chanrion, Olivier; Neubert, Torsten

Published in:
Geophysical Research Letters

Link to article, DOI:
10.1002/2016GL072216

Publication date:
2017

Document Version
Publisher's PDF, also known as Version of record

AGU PUBLICATIONS

Geophysical Research Letters

RESEARCH LETTER
10.1002/2016GL072216

Key Points:
- After the end of the streamer collision, the field at the tips of the newly formed double-headed streamer gets elevated
- The electron motion remains quasi-isotropic despite the large enhanced field observed during the collision
- During the encounter the exponential energy distribution above 150 eV has a characteristic size of 40 eV

Supporting Information:
- Supporting Information S1
- Movie S1
- Movie S2
- Movie S3
- Movie S4

Correspondence to:
C. Köhn,
koehn@space.dtu.dk

Citation:
Köhn, C., O. Chanrion, and T. Neubert (2017), Electron acceleration during streamer collisions in air, *Geophys. Res. Lett.*, *44*, 2604–2613, doi:10.1002/2016GL072216.

Received 9 DEC 2016
Accepted 28 FEB 2017
Accepted article online 6 MAR 2017
Published online 15 MAR 2017

Electron acceleration during streamer collisions in air

Christoph Köhn[1], Olivier Chanrion[1], and Torsten Neubert[1]

[1] DTU Space, National Space Institute, Technical University of Denmark, Kongens Lyngby, Denmark

Abstract High-voltage laboratory experiments show that discharges in air, generated over a gap of one meter with maximal voltage of 1 MV, may produce X-rays with photon energies up to 1 MeV. It has been suggested that the photons are bremsstrahlung from electrons accelerated by the impulsive, enhanced field during collisions of negative and a positive streamers. To explore this process, we have conducted the first self-consistent particle simulations of streamer encounters. Our simulation model is a 2-D, cylindrically symmetric, particle-in-cell code tracing the electron dynamics and solving the space charge fields, with a Monte Carlo scheme accounting for collisions and ionization. We present the electron density, the electric field, and the velocity distribution as functions of space and time. Assuming a background electric field 1.5 times the breakdown field, we find that the electron density reaches $2 \cdot 10^{21}$ m^{-3}, the size of the encounter region is $\sim 3 \cdot 10^{-12}$ m^3 and that the field enhances to ~9 times the breakdown field during $\sim 10^{-11}$ s. We further find that the radial component becomes comparable to the parallel component, which together with angular scattering leads to an almost isotropic distribution of electrons. This is consistent with laboratory observations that X-rays are emitted isotropically. However, the maximum energy of electrons reached in the simulation is ~600 eV, which is well below the energies required to explain observations. The reason is that the encounter region is small in size and duration. For the photon energies observed, the field must be enhanced in a larger region and/or for a longer time.

1. Introduction

In 1994, bursts of gamma rays from thunderstorms were detected from the Compton Gamma Ray Observatory satellite [*Fishman et al.*, 1994]. The discovery was later confirmed by measurements from other satellites [*Smith et al.*, 2005; *Briggs et al.*, 2010; *Marisaldi et al.*, 2010; *Tavani et al.*, 2011; *Briggs et al.*, 2013; *Østgaard et al.*, 2015; *Gjesteland et al.*, 2015; *Chronis et al.*, 2015] that gave details of the energy spectrum and documenting that these terrestrial gamma-ray flashes (TGFs) have photon energies of up to 40 MeV [*Marisaldi et al.*, 2014]. While TGFs were first thought to be associated with high-altitude lightning in the stratosphere and mesosphere, they were later shown to be associated with lighting inside the clouds [*Østgaard et al.*, 2008; *Hazelton et al.*, 2009; *Cummer et al.*, 2014].

High-energy photon beams have also been observed in laboratory discharges mimicking lightning on a much shorter spatial scale [*Babich*, 2003; *Nguyen et al.*, 2008; *Rahman et al.*, 2008; *March and Montanyà*, 2010; *Shao et al.*, 2011; *Kochkin et al.*, 2012, 2014; *Montanyà et al.*, 2015]. In recent work laboratory discharges with a peak voltage of 1 MV in a 1 m gap between the electrodes have been observed to produce X-rays with energies of up to 1 MeV and with characteristic energy of 160 keV emitted isotropically from the location of the discharge [*Kochkin et al.*, 2016].

The TGFs from lightning and the radiation from laboratory discharges are processes that both are generated in a two-step process: first, electrons are accelerated to high energies, then they scatter at air molecules producing photons through the bremsstrahlung process [*Fishman et al.*, 1994; *Torii et al.*, 2004; *Dwyer*, 2012; *Xu et al.*, 2012a]. For the acceleration of electrons in thunderstorms there are currently two classes of theories. One considers a larger region surrounding the cloud where the electric field drives relativistic runaway electron avalanches seeded by electrons with energies in the runaway regime created by cosmic ray ionization of the atmosphere [*Wilson*, 1925; *Gurevich et al.*, 1992; *Dwyer*, 2007, 2012; *Babich et al.*, 2012; *Gurevich and Karashtin*, 2013]. In the other theory, electrons are accelerated in the streamer-leader process in a smaller region of high electric field around the lightning leader tip [*Carlson et al.*, 2010; *Babich et al.*, 2011; *Celestin and Pasko*, 2011; *Xu et al.*, 2012a; *Köhn et al.*, 2014; *Köhn and Ebert*, 2015].

In laboratory discharges electrons are accelerated in the high field tips of streamers [*Moss et al.*, 2006; *Dwyer et al.*, 2008; *Li et al.*, 2009; *Chanrion and Neubert*, 2010]. *Cooray et al.* [2009] propose that the encounter of two oppositely polarized streamers can enhance the electric field for electrons to gain enough energy to produce observed X-rays. They consider discharges in an 80 cm long, rod-sphere air gap with voltages between 850 kV and 980 kV which they also investigated experimentally [*Rahman et al.*, 2008]. They estimate theoretically that for distances of 5 mm to 5 cm between two encountering streamer heads, electrons can gain energies between ~100 keV and ~400 keV, which is sufficiently high to produce the X-rays reported in *Rahman et al.* [2008].

Ihaddadene and Celestin [2015] were the first to investigate the emission of X-rays related to the encounter of streamers. They use a two-step approach: first, they calculate the motion of two colliding streamers with a fluid code to determine the temporal evolution of the electron density and the electric field distribution. In the second step they insert test electrons with an initial energy of 1 eV in the (time varying) electric field and simulate their acceleration and collisional interactions with a Monte Carlo code. They assume a background electric field of approximately 1.5 times the breakdown field and find that the encounter only will produce few photons with energies above 1 keV. The approach, however, does not inject electrons self-consistently with the streamer formation and does not account for the formation of space charges created through ionization by the test electrons.

Here we present, for the first time, self-consistent simulations of streamer encounters using a particle-in-cell code, following the electrons of the streamers and updating the electric field, coupled with a Monte Carlo scheme that account for collisional interactions and photoionization. Hence, we are able to resolve the effect of all space charges on the electric field and to follow the acceleration of cold electrons in the streamer front.

A brief introduction of our model is presented in section 2. In section 3 we present and discuss our results on the electric field and density distributions, and on the electron velocity distributions in the encounter region. Finally we summarize and conclude in section 4.

2. The Model

For our simulations we use a particle-in-cell (PIC) Monte Carlo code with cylinder symmetric domain. The size of the domain is $(L_r, L_z) = (1.25, 14)$ mm and has 150 grid points in r and 1200 grid points in z. After every time step we solve Poisson's equation for the electric potential induced by local space charges and from the potential we determine the electric field. At the boundaries $(z = 0, L_z)$ we use the Dirichlet boundary conditions $\phi(r, 0) = 0$ and $\phi(r, L_z) = E_{\mathrm{amb}} \cdot L_z$ where E_{amb} is the ambient electric field, and at $(r = 0, L_r)$ we use Neumann boundary conditions with $\partial\phi/\partial r = 0$.

The two streamers are initiated by two equal charge-neutral ionization patches of cold electrons in a Gaussian density distribution with a peak electron (and ion) density of 10^{20} m^{-3} and an exponential width of 0.2 mm. The two patches are centered on the axis of symmetry at $L_z = 5.5$ mm and at 9 mm. The atmosphere is at standard temperature and pressure consisting of oxygen and nitrogen molecules with a number density of $2.547 \cdot 10^{25}$ m^{-3}. The ambient electric field is 1.5 E_k, where $E_k \approx 32$ kV cm^{-1} is the classical breakdown field. Note that the electric field of a bidirectional streamer is slightly smaller than of a single-headed streamer [see, e.g., *Qin et al.*, 2012]. For an overview of the collision processes and photoionization electrons we refer to [*Chanrion and Neubert*, 2008; *Köhn et al.*, 2017].

Because of the growing number of electrons, we use an adaptive particle scheme whereby electrons may be merged, conserving the charge distribution as well as the electron energy and momentum [*Chanrion and Neubert*, 2008]. The scheme merges electrons cellwise, i.e., two electrons are merged only if they are within the grid size of one cell. This method takes into account the local nature of streamers with intense ionization waves in the streamer heads. Within one cell, we minimize numerical effects originating from merging electrons with different energies, by merging two electrons only if they are close in energy space. To resolve high-energy electrons and electrons within barely populated cells, we have also implemented a splitting scheme. Super-electrons with energies above 150 eV and super-electrons solely populating one cell are split leading to maximal 100 new computer-electrons with reduced weight.

We note that the setup of our simulation only covers a small cutout of the whole discharge process, namely, the motion of two encountering streamers within a few millimeter distance. In reality discharges consist of multiple streamers [*Kochkin et al.*, 2014]. Hence, in our simulation, we are not able to resolve the electric field

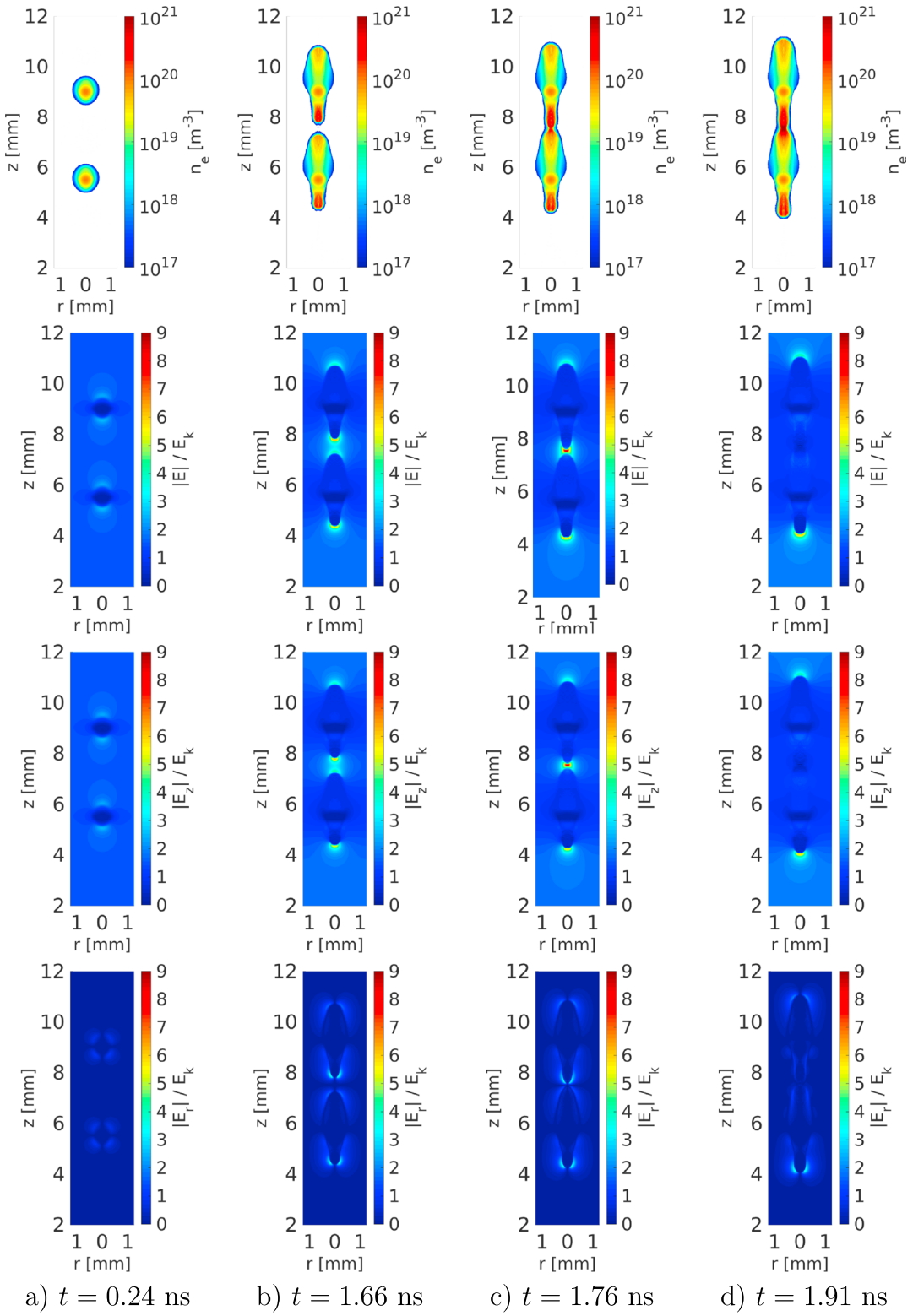

Figure 1. (first row) The electron density, (second row) the absolute value of the electric field, (third row) E_z, and (fourth row) E_r at different time steps.

profile induced by the interaction of more than two streamers. We cannot exclude that the electric field reaches higher or lower or that the duration of high electric fields is longer than we will discuss in the next section. However, as in *Ihaddadene and Celestin* [2015], we have already chosen a high ambient field compared to experiments [*Nijdam et al.*, 2010] to maximize the probability of X-ray emission. Besides the missing influence among several streamers, also the electron number in our simulation is much less than the electron number in a whole discharge.

3. Results

3.1. Streamer Formation and Encounter

The electron density and the electric field are shown at different time steps in Figure 1. Figure 1 (first row) shows density and the following rows the total electric field E and its components E_z and E_r. The background electric field is directed downward. Starting from two electron patches (a), two bidirectional streamers form (b) where the upper halves are negative and the lower halves positive streamers. The two approaching streamer fronts meet after approximately 1.76 ns (c) and have collapsed at the end of the simulation at 1.91 ns (d). We provide an animation of the streamer evolution up to 2.1 ns in the supporting information.

We see that the positive fronts carry a higher electron density and propagate with a smaller front radius than the negative fronts. After the formation of the bidirectional streamers and before the encounter, the total field at the negative fronts reaches approximately 4.5 E_k and at the positive fronts 5.5 E_k. During the encounter (c), the field between the two streamers reaches almost 9 E_k, declining to 2 E_k after 0.02 ns.

It is custom to discuss runaway electron acceleration under the simplistic assumption that the electron motion and its acceleration are aligned with the electric field (forward scattering). In this view, all electrons are in the runaway regime with an electric field magnitude of approximately $8E_k$, e.g., the force of the electric field acting on electrons is larger than the frictional force of air molecules. However, we have previously shown that angular scattering is important and places severe limitations on the production of runaway electrons [*Chanrion et al.*, 2016]. We will return to this point in the following subsection when we present the results on the electron velocity distribution.

Figures 1 (third row) and 1 (fourth row) show E_z and E_r. We see that when the streamers have formed, and before the encounter (b), E_z is larger than E_r as expected, but note that at the positive streamer front (with the highest electron density) the r component reaches comparable values, with $E_r \sim 3.5\ E_k$ and $E_z \sim 4.5E_k$. We return also to this point in the following subsection.

The velocities of the two encountering streamer fronts are compared to the velocities of the two heads of a single bidirectional streamer in Figure 2a. For that purpose we initiated the single bidirectional streamer from one electron-ion patch placed at 7 mm with the same Gaussian density distribution and ambient field as for the initial two charge-neutral ionization patches. For both cases, the single bidirectional streamer and the two encountering streamers, we have calculated the velocity as a change in the position of the peak electric fields of the moving (and encountering) streamer fronts. After the streamer formation phase, all fronts propagate with an increasing velocity, the negative fronts with a higher velocity than the positive ones consistent with past work [*Luque et al.*, 2008; *Naidis*, 2009; *Qin and Pasko*, 2014]. We also see that the colliding streamers accelerate faster than the single ones after $\approx$1 ns, giving the appearance of mutual attraction between the two opposite polarity streamer fronts. It implies that at this point in time, the electric field of one front reaches to the other and adds to it, thereby increasing the total field of the fronts, which leads to faster propagation velocities [*Briels et al.*, 2008]. At this time the two attracting fronts are approximately within 2 mm from each other.

3.2. During the Encounter

We now take a closer look at the encounter region where the electric field reaches its highest values and discuss the acceleration of electrons in that region. First, we look at the size of the region with high field and estimate the number of electrons it contains.

The electron density and the electric field in the r, z plane from $z = 7-8$ mm are shown in Figure 3 just before, during, and after the encounter. The positive streamer (propagating downward) carries densities reaching $\sim 10^{21}$ m^{-3} with the negative streamer reaching $\sim 10^{20}$ m^{-3}. When the streamers have combined (Figure 3, bottom row), the region of high electron density reaches its maximum extent of about 0.1 mm in the radial

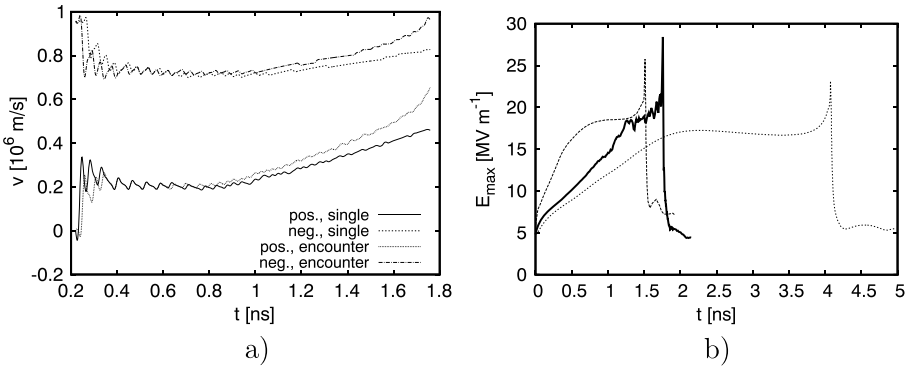

Figure 2. (a) The velocity of the negative and of the positive streamer fronts of a single streamer and of two approaching streamers as a functions of time. (b) The maximum electric field E_{max} as a function of time for the encounter region in our simulations (full) and for the whole simulation domain for *Ihaddadene and Celestin* [2015] (dash dotted).

direction and 0.2 mm in the axial direction for a volume of $\sim 6 \cdot 10^{-12}$ m^3. With an estimated density of $\sim 5 \cdot 10^{20}$ m^{-3} we find the number of electrons in the volume to be $\sim 3 \cdot 10^9$. The electric field intensifies at the encounter reaching values above those of a single positive streamer ($\sim 5E_k$) in a region approximately half of the volume of the high density region or $\sim 3 \cdot 10^{-12}$ m^3. The field maximizes at the encounter, driving high ionization rates which leads to the higher electron density, which in turn shorts the field as in [*Ihaddadene and Celestin*, 2015]. This is why the field maximum (Figure 3, middle row) occurs before the density maximum (Figure 3, bottom row).

The on-axis density and electric field in the encounter region are shown in Figure 4. The plots allow us to read off more precise values of the fields and densities, which maximize on the axis. We see that during the encounter (Figure 4, second panel) the density peaks at $\sim 6 \cdot 10^{20}$ m^{-3} and the electric field at $\sim 9\, E_k$ while after additional 0.02 ns, the density has increased to $\sim 2 \cdot 10^{21}$ m^{-3} and the electric field decreased to a maximum of $\sim 3\, E_k$. The full temporal evolution of the on-axis electric field up to 2.1 ns is added as the supporting information which is similar to the material provided by *Ihaddadene and Celestin* [2015]. In contrast to their work, however, we provide the electric field of two bidirectional streamers which gives a detailed view on the field between the streamer tips of the encounter region and of the streamer tips close to the simulation boundaries.

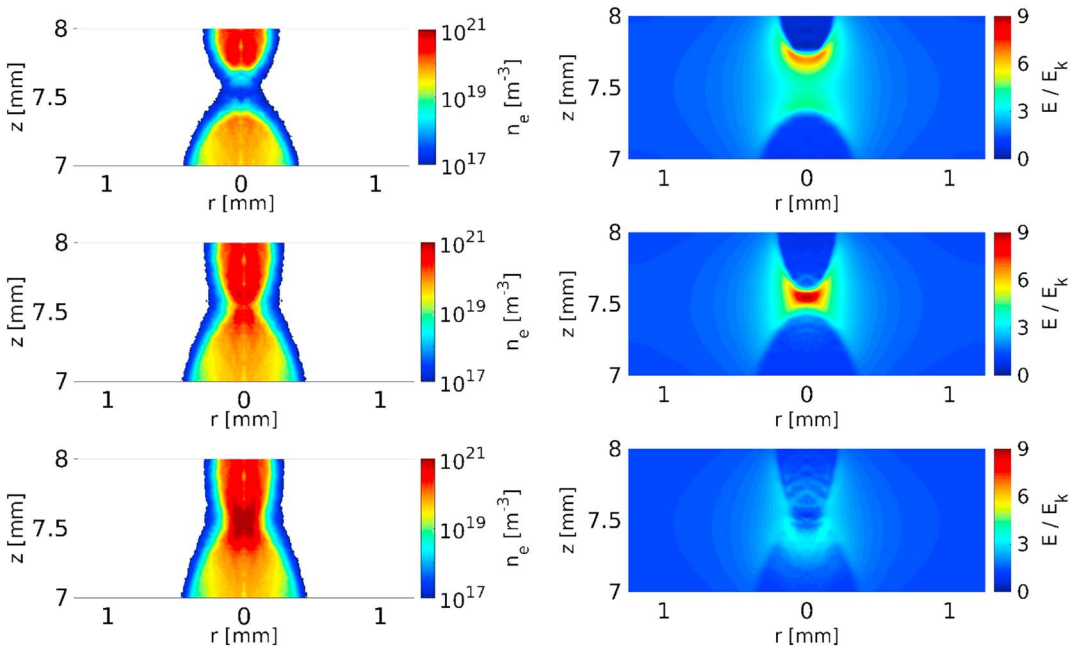

Figure 3. A close-up of the region $z = 7$–8 mm. The electron density is in the left column and the total electric field in the right column. (top row) $t = 1.71$, (middle row) 1.76, and (bottom row) 1.78 ns.

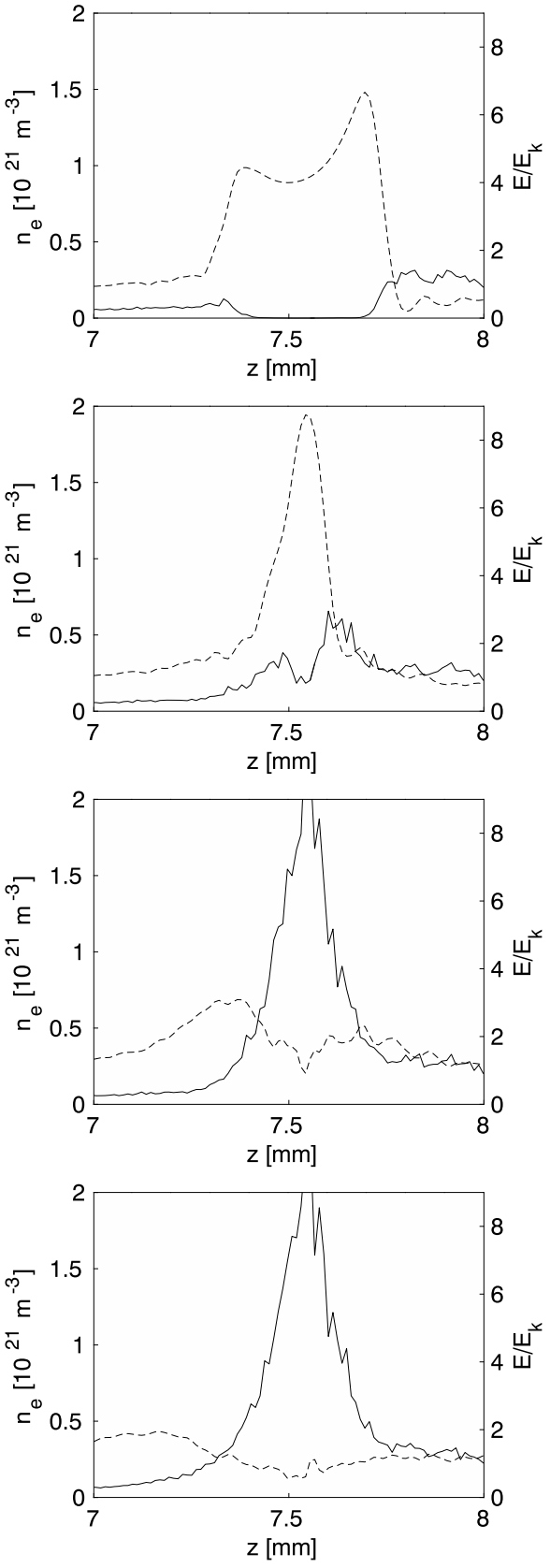

Figure 4. The density (solid) and electric field (dashed) along the z axis for $z = 7-8$ mm. (first panel) $t = 1.71$, (second panel) 1.76, (third panel) 1.78, and (fourth panel) 1.83 ns.

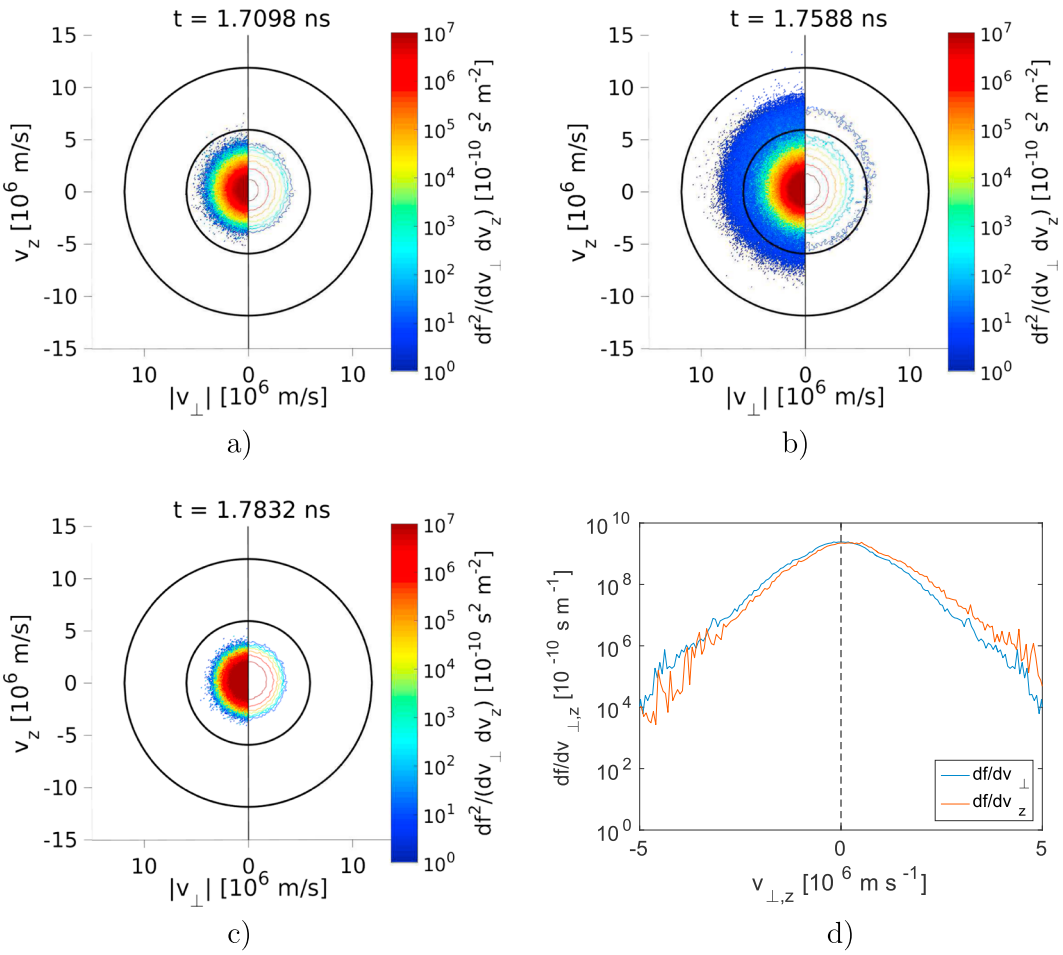

Figure 5. The two-dimensional electron distribution $d^2f/(dv_\perp dv_z)$ in velocity space in the region $z = 7-8$ mm after (a) $t = 1.71$, (b) 1.76, and (c) 1.78 ns as well as (d) the integrated velocity distribution $df/dv_{\perp,z}$ after 1.76 ns. In addition, the right halves of Figures 5a–5c show isocontour lines of the electron distribution.

We observe that before the encounter, there is a strongly reduced electric field between the encountering region and the outer streamer tips. Additionally, we also observe that not only in the encounter region but also at the streamer tips the field increases and that the field at these streamer stays between $4E_k$ and $6E_k$ even after the collapse of the field in the encounter region.

The electron velocity distribution $d^2f/(dv_z dv_\perp)$ for electrons in the range $z = 7-8$ mm is shown in Figure 5a–5c. The black circles are equi-energy curves at 100 eV and 400 eV. Just before the encounter the electron velocities are limited to below $\sim 5 \cdot 10^6$ m/s (~70 eV) and at the encounter, the electron number grows and their velocity doubles with a few electrons reaching $15 \cdot 10^6$ m/s or 640 eV. After the encounter, and within 0.02 ns, their velocities decline to before the encounter, while their number density remains high. As supporting information we have added a movie of the velocity distribution of electrons in the encounter region up to 2.1 ns.

The right halves of Figures 5a–5c show the isocontour lines of the velocity distribution. Whereas the electron distribution is isotropic after 1.71 ns and 1.78 ns, the motion of electrons with energies of above 100 eV after 1.76 ns is slightly shifted into the forward direction. Figure 5d shows the velocity distributions $df/dv_{\perp,z}$ along $v_\perp$ or along v_z. It shows that the velocity distribution perpendicular to the ambient field is symmetric whereas the velocity distribution parallel to the ambient field is slightly asymmetric. Because of the high field magnitude in z direction, the overall isotropy of the velocity distribution is perhaps surprising but is caused by the significant magnitude of the radial component of the electric field and of angular scattering, as mentioned in the previous subsection, combined with a too short duration of the field enhancement. This is consistent with the laboratory observations that bremsstrahlung photons in their discharges appear to be emitted isotropically [*Kochkin et al.*, 2016].

The maximum electric field in the encounter region as a function of time is shown in Figure 2b together with the maximum fields in the whole simulation domain of *Ihaddadene and Celestin* [2015]. Whereas we have used a background field of 48 kV cm^{-1}, Ihaddadene and Celestin used 40 kV cm^{-1} (dotted) and 60 kV cm^{-1} (dashed). The curves show a general agreement between our PIC approach and their fluid approach, e.g., a very narrow peak in the field followed by a sudden drop. From the time sequence we estimate that the time the electric field is above the value of a single positive streamer ($\sim 5\ E_k$) is less than $1 \cdot 10^{-11}$s. A difference that may be important is that after the coalescence of the streamers, the electric field remains high and close to $2\ E_k$ within ≈100 ps after the encounter in a larger region as seen in Figures 3 and 4.

4. Discussion and Conclusions

We are now prepared to discuss the maximum electron acceleration expected in the encounter, e.g., with no scattering from ambient molecules, and to compare those to the actual acceleration shown in Figure 5. We estimated the maximum spatial dimension of the high-field region to 0.1 mm, the maximum temporal duration to 0.01 ns and the field maximum to 28 MV m^{-1}. Assuming that the average, effective values are really only half of that, we find that the energy gain of acceleration across the region, $E_{\max} \mathrm{d}z$, which gives ∼700 eV, or alternatively that the velocity gain during the time of acceleration, $\mathrm{d}v = \sim q/m * E_{\max} \mathrm{d}t$, is ∼430 eV. These energy values are consistent with the energies of electrons reached in the particle code. Note that we split all computer electrons with energies above 150 eV, and as such, they represent single real electrons. After 1.76 ns there are 33194 electrons with energies above 150 eV, 9 electrons above 400 eV, and 1 electron above 500 eV; the energy distribution above 150 eV can be fitted by an exponential $\sim \exp(E/E_0)$ with a characteristic energy of approximately 40 eV.

This result implies that the acceleration of two colliding streamers, relative to acceleration in a single streamer front, is quite modest because of the small encounter region and the short duration of an encounter. On the other hand, we estimated the number of electrons in the encounter zone to $\sim 3 \cdot 10^9$ but sample these with computer electrons representing up to eight million real electrons and therefore do not represent the finite probability that a few electrons may reach energies of 150 eV and higher into the keV regime. We note that after the encounter, our field remains at a relative high value of $\sim 2\ E_k$ in a larger region (Figures 3 and 4) within ≈ 100 ps in contrast to the results of *Ihaddadene and Celestin* [2015] where the field drops below E_k within ≈ 50 ps; thus, if electrons reach above the conventional threshold energy at that electric field, which is ∼3 keV, further acceleration outside of the encounter zone is possible. The temporal evolution of the on-axis field demonstrates that in contrast to the work of *Ihaddadene and Celestin* [2015], the electric fields at the tips of the newly formed double-headed streamer get elevated after the decline of the field in the encounter region. The field values of above $4\ E_k$ on the negative side and $6\ E_k$ on the positive side might provide further acceleration of electrons in the vicinity of the streamer tips.

We note here that the appearance of high-energy electrons in simulations depends also on the particle management. We may, therefore, even with a particle code, have missed the few electrons needed to enter the runaway regime.

With the above in mind, we may also suggest that a larger background electric field than adopted here ($1.5\ E_k$) would lead to the energies required to explain experiments. Such fields could, for instance, be present close to leader or space leader tips.

Ihaddadene and Celestin have used a simulation setup similar to ours, but instead of simulating the collision of two encountering streamers with a particle-in-cell code, they use a plasma fluid code and do not resolve individual electrons, present the electron energy distribution or make a statement about the degree of isotropy. They estimate that during the encounter at most 2000 out of $13 \cdot 10^9$ electrons gain energies above 1 keV and that subsequently in average only 0.02 X-rays with energies above 1 keV can be produced. Note that they set the electric field such that the emission of X-rays is maximized. The rest of the electrons are supposed to have energies below 1 keV which is consistent with our estimations.

Finally, we observe that the current configuration is not suitable to produce sufficiently many electrons with energies above 1 keV and subsequently X-rays with energies above the same energy where the limiting factor is the duration of the collision rather than the peak field (as in *Ihaddadene and Celestin* [2015]). However, we cannot completely exclude the production of high-energy electrons since the appearance of high-energy electrons also depends on the particle management.

Finally, with the particle-in-cell code, we have observed that the electron beam moves almost isotropically between the two encountering streamer fronts, with a slight forward shift for electrons above 100 eV, which gives a hint why X-rays have been measured to be emitted isotropically [*Kochkin et al.*, 2016]. In future work, we will elaborate whether high background fields as they occur in the vicinity of leader tips will lead to the production of a significant X-ray signal.

Acknowledgments
The research was partly funded by the Marie Curie Actions of the European Union's Seventh Framework Programme (FP7/2007-2013) under REA grant agreement 609405(COFUNDPostdocDTU). This work was supported by the European Science Foundation research networking project "Thunderstorm Effects on the Atmosphere-Ionosphere System" (TEA-IS). The simulation code can be obtained from C.K. (koehn@space.dtu.dk).

References

Babich, L. P. (2003), *High-Energy Phenomena in Electric Discharges in Dense Gases: Theory, Experiment and Natural Phenomena, ISTC Sci. Technol. Ser.*, vol. 2, 358 pp., Futurepast, Arlington, Va.

Babich, L. P., et al. (2011), Self-sustained relativistic runaway electron avalanches in transverse field of lightning leader as a source of terrestrial gamma-ray flashes, *JETP Lett.*, *94*, 606–609.

Babich, L. P., E. I. Bochkov, J. R. Dwyer, and I. M. Kutsyk (2012), Numerical simulations of local thundercloud field enhancements caused by runaway avalanches seeded by cosmic rays and their role in lightning initiation, *J. Geophys. Res.*, *117*, A09316, doi:10.1029/2012JA017799.

Briels, T. M. P., J. Kos, G. J. J. Winands, E. M. van Veldhuizen, and U. Ebert (2008), Positive and negative streamers in ambient air: Measuring diameter, velocity and dissipated energy, *J. Phys. D Appl. Phys.*, *41*, 234004.

Briggs, M. S., et al. (2010), First results on terrestrial gamma ray flashes from the Fermi Gamma-ray Burst Monitor, *J. Geophys. Res.*, *115*, A07323, doi:10.1029/2009JA015242.

Briggs, M. S., et al. (2013), Terrestrial gamma-ray flashes in the Fermi era: Improved observations and analysis methods, *J. Geophys. Res. Space Physics*, *118*, 3805–3830, doi:10.1002/jgra.50205.

Carlson, B. E., N. G. Lehtinen, and U. S. Inan (2010), Terrestrial gamma ray flash production by active lightning leader channels, *J. Geophys. Res.*, *115*, A10324, doi:10.1029/2010JA015647.

Celestin, S., and V. P. Pasko (2011), Energy and fluxes of thermal runaway electrons produced by exponential growth of streamers during the stepping of lightning leaders and in transient luminous events, *J. Geophys. Res.*, *116*, A03315, doi:10.1029/2010JA016260.

Chanrion, O., and T. Neubert (2008), A PIC-MCC code for simulation of streamer propagation in air, *J. Comput. Phys.*, *227*, 7222–7245.

Chanrion, O., and T. Neubert (2010), Production of runaway electrons by negative streamer discharges, *J. Geophys. Res.*, *115*, A00E32, doi:10.1029/2009JA014774.

Chanrion, O., Z. Bonaventura, A. Bourdon, and T. Neubert (2016), Influence of the angular scattering of electrons on the runaway threshold in air, *Plasma Phys. Controlled Fusion*, *58*, 044001.

Chronis, T., et al. (2015), Characteristics of thunderstorms that produce terrestrial gamma-ray flashes, *Bull. Am. Meteorol. Soc.*, *14*, 639–653, doi:10.1175/BAMS-D-14-00239.1.

Cooray, V., L. Arevalo, M. Rahman, J. Dwyer, and H. Rassoul (2009), On the possible origin of X-rays in long laboratory sparks, *J. Atmos. Sol. Terr. Phys.*, *71*, 1890–1898.

Cummer, S. A., et al. (2014), The source altitude, electric current, and intrinsic brightness of terrestrial gamma ray flashes, *Geophys. Res. Lett.*, *41*, 8586–8593, doi:10.1002/2014GL062196.

Dwyer, J. R. (2007), Relativistic breakdown in planetary atmospheres, *Phys. Plasmas*, *14*, 042901.

Dwyer, J. R. (2012), The relativistic feedback discharge model of terrestrial gamma ray flashes, *J. Geophys. Res.*, *117*, A02308, doi:10.1029/2011JA017160.

Dwyer, J. R., Z. Saleh, H. K. Rassoul, D. Concha, M. Rahman, V. Cooray, J. Jerauld, M. A. Uman, and V. A. Rakov (2008), A study of X-ray emission from laboratory sparks in air at atmospheric pressure, *J. Geophys. Res.*, *113*, D23207, doi:10.1029/2008JD010315.

Fishman, G. J., et al. (1994), Discovery of intense gamma-ray flashes of atmospheric origin, *Science*, *264*, 1313–1316.

Gjesteland, T., N. Østgaard, S. Laviola, M. M. Maglietta, E. Arnone, M. Marisaldi, F. Fuschino, A. B. Collier, F. Fabró, and J. Montanya (2015), Observation of intrinsically bright terrestrial gamma ray flashes from the Mediterranean basin, *J. Geophys. Res. Atmos.*, *120*, 12,143–12,156, doi:10.1002/2015jd023704.

Gurevich, A. V., and A. N. Karashtin (2013), Runaway breakdown and hydrometeors in lightning initiation, *Phys. Rev. Lett.*, *110*, 185005.

Gurevich, A. V., G. Milikh, and R. Roussel-Dupré (1992), Runaway electron mechanism of air breakdown and preconditioning during a thunderstorm, *Phys. Lett. A*, *165*, 463–468.

Hazelton, B. J., et al. (2009), Spectral dependence of terrestrial gamma-ray flashes on source distance, *Geophys. Res. Lett.*, *36*, L01108, doi:10.1029/2008GL035906.

Ihaddadene, M. A., and S. Celestin (2015), Increase of the electric field in head-on collisions between negative and positive streamers, *Geophys. Res. Lett.*, *42*, 5644–5651, doi:10.1002/2015GL064623.

Kochkin, P. O., C. V. Nguyen, A. P. J. van Deursen, and U. Ebert (2012), Experimental study of hard X-rays emitted from metre-scale positive discharges in air, *J. Phys. D Appl. Phys.*, *45*, 425202.

Kochkin, P. O., A. P. J. van Deursen, and U. Ebert (2014), Experimental study of the spatio-temporal development of metre-scale negative discharge in air, *J. Phys. D Appl. Phys.*, *47*, 145203.

Kochkin, P. O., C. Köhn, A. P. J. van Deursen, and U. Ebert (2016), Analyzing X-ray emissions from meter-scale negative discharges in ambient air, *Plasma Sources Sci. Technol.*, *25*, 044002.

Köhn, C., and U. Ebert (2015), Calculation of beams of positrons, neutrons, and protons associated with terrestrial gamma ray flashes, *J. Geophys. Res. Atmos.*, *120*, 1620–1635, doi:10.1002/2014JD022229.

Köhn, C., U. Ebert, and A. Mangiarotti (2014), The importance of electron-electron Bremsstrahlung for terrestrial gamma-ray flashes, electron beams and electron-positron beams, *J. Phys. D Appl. Phys.*, *47*, 252001. Fast Track Communication.

Köhn, C., O. Chanrion, and T. Neubert (2017), The influence of bremsstrahlung on electric discharge streamers in N_2, O_2 gas mixtures, *Plasma Sources Sci. Technol.*, *26*, 015006.

Li, C., U. Ebert, and W. Hundsdorfer (2009), 3D hybrid computations for streamer discharges and production of runaway electrons, *J. Phys. D Appl. Phys.*, *42*, 202003. Fast Track Communication.

Luque, A., V. Ratushnaya, and U. Ebert (2008), Positive and negative streamers in ambient air: Modelling evolution and velocities, *J. Phys. D Appl. Phys.*, *41*, 234005.

March, V., and J. Montanyà (2010), Influence of the voltage-time derivative in X-ray emission from laboratory sparks, *Geophys. Res. Lett.*, *37*, L19801, doi:10.1029/2010GL044543.

Marisaldi, M., et al. (2010), Detection of terrestrial gamma ray flashes up to 40 MeV by the AGILE satellite, *J. Geophys. Res.*, *115*, A00E13, doi:10.1029/2009JA014502.

Marisaldi, M., et al. (2014), Properties of terrestrial gamma ray flashes detected by AGILE MCAL below 30 MeV, *J. Geophys. Res. Space Physics*, *119*, 1337–1355, doi:10.1002/2013JA019301.
Montanyà, J., F. Fabró, V. March, O. van der Velde, G. Solà, D. Romero, and O. Argemí (2015), X-rays and microwave RF power from high voltage laboratory sparks, *J. Atmos. Sol. Terr. Phys.*, *136*, 94–97.
Moss, G. D., V. P. Pasko, N. Liu, and G. Veronis (2006), Monte Carlo model for analysis of thermal runaway electrons in streamer tips in transient luminous events and streamer zones of lightning leaders, *J. Geophys. Res.*, *111*, A02307, doi:10.1029/2005JA011350.
Naidis, G. V. (2009), Positive and negative streamers in air: Velocity-diameter relation, *Phys. Rev. E*, *79*, 057401.
Nguyen, C. V., A. P. J. van Deursen, and U. Ebert (2008), Multiple X-ray bursts from long discharges in air, *J. Phys. D Appl. Phys.*, *41*, 234012.
Nijdam, S., G. Wormeester, E. M. van Veldhuizen, and U. Ebert (2010), Probing background ionization: positive streamers with varying pulse repetition rate and with a radioactive admixture, *J. Phys. D Appl. Phys.*, *44*, 455201.
Østgaard, N., J. Stadsnes, P. H. Connell, and B. Carlson (2008), Production altitude and time delays of the terrestrial gamma flashes: Revisiting the Burst and Transient Source Experiment spectra, *J. Geophys. Res.*, *113*, A02307, doi:10.1029/2007JA012618.
Østgaard, N., K. H. Albrecthsen, T. Gjesteland, and A. Collier (2015), A new population of terrestrial gamma-ray flashes in the RHESSI data, *Geophys. Res. Lett.*, *42*, 10,937–10,942, doi:10.1002/2015GL067064.
Qin, J., and V. P. Pasko (2014), On the propagation of streamers in electrical discharges, *J. Phys. D Appl. Phys.*, *47*, 435202.
Qin, J., S. Celestin, and V. P. Pasko (2012), Formation of single and double-headed streamers in sprite-halo events, *Geophys. Res. Lett.*, *39*, L05810, doi:10.1029/2012GL051088.
Rahman, M., V. Cooray, N. A. Ahmad, J. Nyberg, V. A. Rakov, and S. Sharma (2008), X-rays from 80 cm long sparks in air, *Geophys. Res. Lett.*, *35*, L06805, doi:10.1029/2007GL032678.
Shao, T., C. Zhang, Z. Niu, P. Yan, V. F. Tarasenko, E. K. Baksht, A. G. Burahenko, and Y. V. Shut'ko (2011), Diffuse discharge, runaway electron and X-ray in atmospheric pressure air in a inhomogeneous electrical field in repetitive pulsed modes, *Appl. Phys.*, *98*, 021506.
Smith, D. M., L. I. Lopez, R. P. Lin, and C. P. Barrington-Leigh (2005), Terrestrial gamma-ray flashes observed up to 20 MeV, *Science*, *307*, 1085–1088.
Tavani, M., et al. (2011), Terrestrial gamma-ray flashes as powerful particle accelerators, *Phys. Rev. Lett.*, *106*, 018501.
Torii, T., T. Nishijima, Z. I. Kawasaki, and T. Sugita (2004), Downward emission of runaway electrons and bremsstrahlung photons in thunderstorm electric fields, *Geophys. Res. Lett.*, *31*, L05113, doi:10.1029/2003GL019067.
Wilson, C. (1925), The electric field of a thundercloud and some of its effects, *Proc. Phys. Soc. London*, *37A*, 32D–37D.
Xu, W., S. Celestin, and V. P. Pasko (2012a), Source altitudes of terrestrial gamma-ray flashes produced by lightning leaders, *Geophys. Res. Lett.*, *39*, L08801, doi:10.1029/2012GL051351.